ELSEVIER

Ceramics International 32 (2006) 157–162

CERAMICS INTERNATIONAL

www.elsevier.com/locate/ceramint

The effect of grain boundary on the properties of $La_{0.7}Sr_{0.3}MnO_3$ thin films prepared by chemical solution deposition

S.M. Liu [a], X.B. Zhu [a], J. Yang [a], W.H. Song [a], J.M. Dai [a], Y.P. Sun [a,b,*]

[a] *Key Laboratory of Materials Physics, Institute of Solid State Physics, Chinese Academy of Sciences, Hefei 230031, PR China*
[b] *National Laboratory of Solid State Microstructures, Nanjing University, Nanjing 210093, PR China*

Received 20 October 2004; received in revised form 11 November 2004; accepted 17 January 2005
Available online 19 March 2005

Abstract

Polycrystalline and epitaxial $La_{0.7}Sr_{0.3}MnO_3$ (LSMO) thin films are fabricated by chemical solution deposition (CSD) method on Si (1 0 0) and $LaAlO_3$ (1 0 0) single crystal substrates, respectively. The transport and magnetic properties of the films are investigated. The magnetoresistance (MR) of LSMO films fabricated on Si (1 0 0) substrates is largely enhanced at low temperatures compared with that of LSMO films on $LaAlO_3$ substrates. The difference of MR properties is discussed in terms of grain boundary (GB) effects.

PACS: 73.50.Dn; 75.47.Lx

Keywords: Manganites; Magnetoresistance; Chemical solution deposition

1. Introduction

Since the colossal magnetoresistance (CMR) effect in the perovskite-doped manganese oxides $R_{1-x}A_xMnO_3$ (R is a trivalent rare-earth element such as La, Nd, or Pr, and A is a divalent dopant such as Ca, Sr, Ba, or Pb) was discovered, it had been extensively investigated in past years not only because of its rich physical properties but also of its potential applications in various devices such as magnetic field sensors and hard disk read heads [1–6].

It is well-known that the material should be in the form of films from the viewpoint of practical applications [7]. As to the fabrication of thin films, the physical deposition methods such as pulse laser deposition (PLD) and magnetron-sputtering (MS) technique can fabricate thin films with good qualities, but they are difficult to fabricate films with large area. The chemical vapor deposition (CVD) method can be easily used to fabricate films with large area, but the precursor is hazardous. Compared with the CVD method, the chemical solution deposition (CSD) is safer. Therefore, it is generally thought that the CSD method is a promising one for the fabrication of manganese oxide thin films with large area [8–10].

It is well-known that Curie temperature of $La_{1-x}Sr_xMnO_3$ is higher than room temperature, implying that it is possible to use magnetoresistance (MR) effect of $La_{1-x}Sr_xMnO_3$ at room temperature [11]. At present, one of the main problems is its small MR value at room temperature under a low applied magnetic field. Hence, many investigations are focused on improving the low field MR (LFMR) of $La_{1-x}Sr_xMnO_3$ materials. Many authors reported that the LFMR could be enhanced remarkably when some weak link grain boundaries (GBs) appeared in CMR materials [12–14]. However, few references are reported about the preparation of $La_{1-x}Sr_xMnO_3$ films using the CSD method, especially as to the effect of GBs on its MR behavior.

In this paper, $La_{0.7}Sr_{0.3}MnO_3$ (LSMO) films are successfully prepared by the CSD method on Si (1 0 0) (denoted LSMO/Si film) and $LaAlO_3$ (1 0 0) (denoted LSMO/LAO film) single crystal substrates. It is found that the substrates play an important role on the structural,

* Corresponding author. Fax: +86 551 559 14 34.
E-mail address: ypsun@issp.ac.cn (Y.P. Sun).

0272-8842/$30.00
doi:10.1016/j.ceramint.2005.01.012

magnetic and transport properties for LSMO films. The LSMO/Si film shows the characteristic of a polycrystalline film, whereas the LSMO/LAO film exhibits the characteristic of an epitaxial film. Moreover, the MR of the LSMO/Si film is largely enhanced at low temperatures compared with that of the LSMO/LAO film, which is suggested to originate from the grain boundary effect.

2. Experimental procedures

For preparation of LSMO thin films, Si (1 0 0) and $LaAlO_3$ (1 0 0) single crystals were chosen as substrates. The solutions of LSMO were synthesized from commercially available chemicals. In brief, stoichiometric amounts of $La(NO_3)_3{\cdot}6H_2O$, $Sr(CH_3COO)_2{\cdot}0.5H_2O$ and $Mn(CH_3COO)_2{\cdot}6H_2O$ were dissolved gradually in a water/ethanol (v/v, 1:9) solution containing citric acid. The molar ratio of metal ions and citric acid was 1:2. Polyethylene glycol (PEG, molecular weight, 20,000) was used as surfactant to prevent the colloidal particles of chelate from aggregation [15,16]. All chemicals used in this work were analytical reagents. The solution was diluted with water and ethanol to a 0.2–0.3 M solution in water/ethanol (v/v, 1:9). The solution was filtered (pore size in filter: 0.2 μm), and the substrates were ultrasonically cleaned using acetone, ethanol and water sequentially. Deposition of LSMO was carried out by a spin-coater at 500 rpm for 5 s, followed by 3000 rpm for 60 s. The as-deposited films were dried at 300 °C for 30 min. The dried films were finally annealed at 900 °C for 2 h under flowing oxygen atmosphere in a quartz tube furnace. In order to obtain the film with the desired thickness, the above spin coating, drying and annealing processes were repeated several times.

A Philips X'pert PRO X-ray diffractormeter (XRD), a Sirion 200 field emission scan electron microscope (FE-SEM) by FED Company and a Park Scientific Instruments designed Autoprobe CP type atomic force micrograph (AFM) were used to characterize the crystallization quality and the microstructure of the films. The temperature dependence of the resistance was measured by the standard four-probe method in the temperature range from 30 to 370 K obtained by means of cryogenic refrigeration equipment. The temperature dependence of magnetization $M(T)$ and the applied magnetic field dependence of the resistance $R(H)$ at different temperatures were measured on a Quantum Design superconducting quantum interference device (SQUID) MPMS system ($2 \leq T \leq 400$ K, $0 \leq H \leq 5$ T).

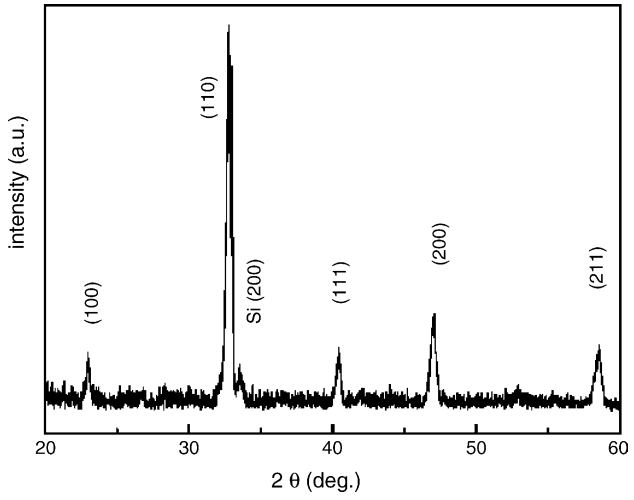

Fig. 1. XRD pattern for the LSMO/Si film.

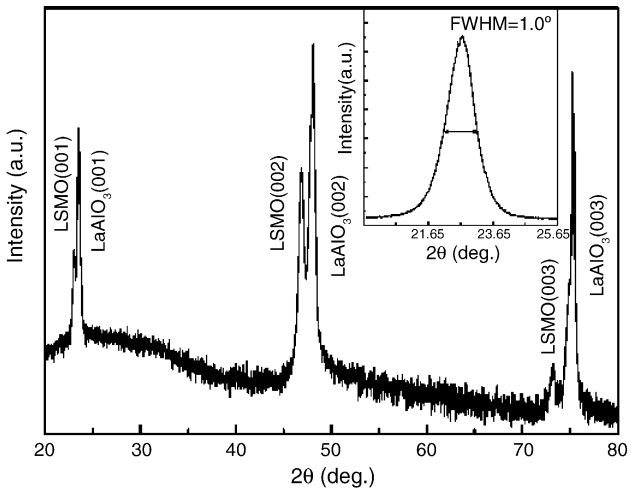

Fig. 2. XRD pattern for the LSMO/LAO film. The inset is the amplification plot of the LSMO (2 0 0) reflection peak.

3. Results and discussion

The standard θ–2θ XRD pattern for the LSMO/Si film is shown in Fig. 1. It exhibits that all diffraction peaks can be indexed to LSMO phase with the pseudocubic structure.

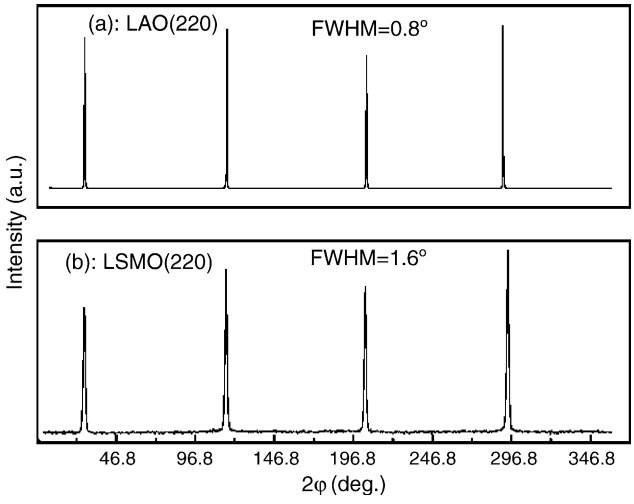

Fig. 3. The XRD in-plane φ scans for $LaAlO_3$ (2 2 0) (a) and LSMO (1 1 0) (b).

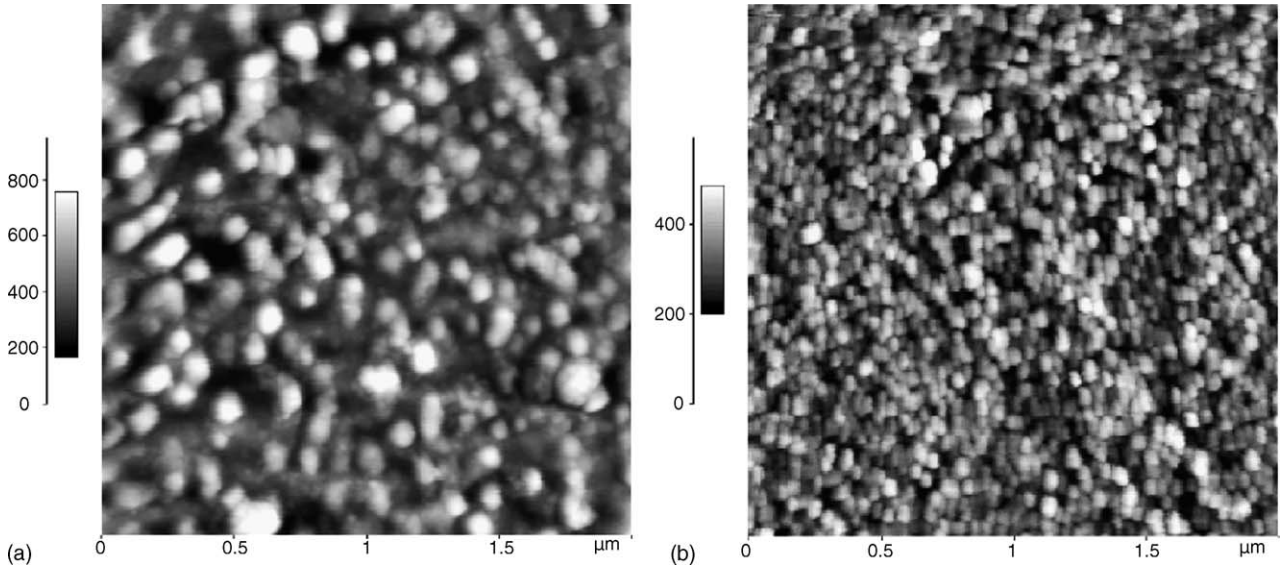

Fig. 4. AFM images for the LSMO/LAO film (a) and the LSMO/Si film (b).

Additionally, it indicates that the LSMO film grows in the form of the polycrystalline film.

Fig. 2 shows the θ–2θ XRD pattern of the LSMO/LAO film. There only exist (h 0 0) peaks attributed to LSMO film besides (h 0 0) peaks of the $LaAlO_3$ substrate, implying that the film is a-axis oriented. The inset of Fig. 2 is the rocking curve result of LSMO (2 0 0) peak. It shows that the full width at half maximum (FWHM) is only about 1.0° indicating that the out-of-plane orientation of the film is rather good. The in-plane φ scan of LSMO (2 2 0) thin film is shown in Fig. 3, which indicates that the LSMO thin film is of the four-fold symmetry and grown on the $LaAlO_3$ substrate in cube-on-cube mode. Considering the FWHM (∼0.8°) of $LaAlO_3$ (2 2 0), the value of FWHM (∼1.6°) of LSMO (2 2 0) indicates that both in-plane and out-of-plane orientations of the film are quite good [17].

The AFM images of both LSMO/LAO and LSMO/Si films are shown in Fig. 4(a) and (b), respectively. Fig. 4(a) exhibits that the LSMO film on $LaAlO_3$ substrates grows in the form of two dimensions (2D) layer-by-layer with faceted surface, which is the typical characteristic of the epitaxial film. However, the LSMO film on Si substrates [Fig. 4(b)] grows in the form of the polyscrystalline film with grain size ranging from 40 to 100 nm. The difference of LSMO growth modes between on Si and $LaAlO_3$ substrates is suggested to originate from the lattice mismatch between the LSMO films and the substrates. The lattice mismatch between the LSMO film and the Si substrate is calculated to be 28% and only −2.57% between the LSMO film and the $LaAlO_3$ substrate.

Fig. 5 shows the FE-SEM images of LSMO/LAO and LSMO/Si films. Fig. 5(a) shows that the LSMO film on the $LaAlO_3$ substrate has dense microstructure and the GBs are

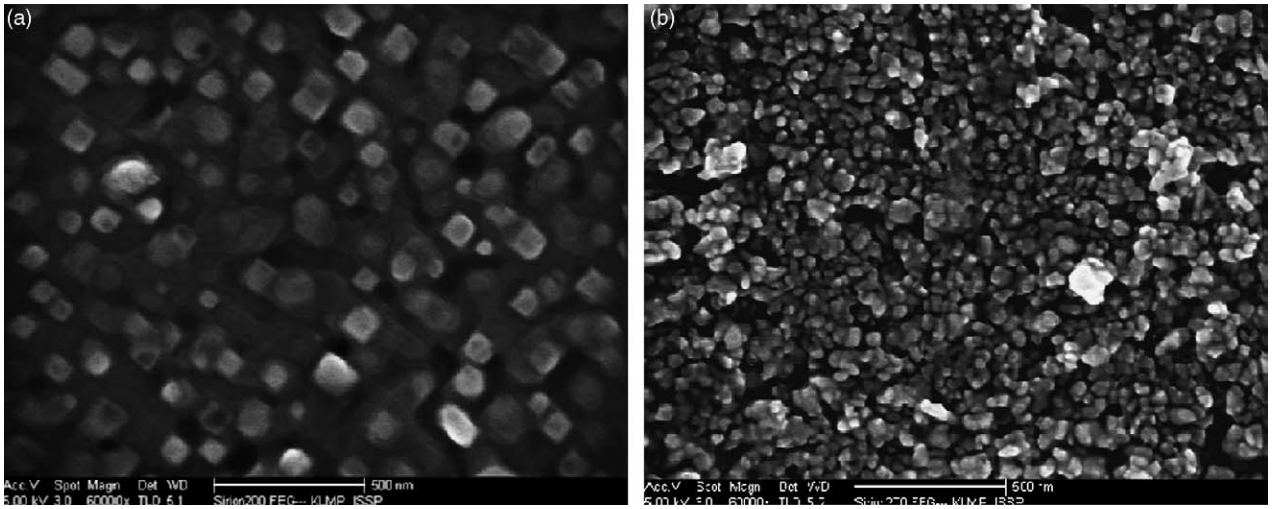

Fig. 5. FE-SEM images for the LSMO/LAO film (a) and the LSMO/Si film (b).

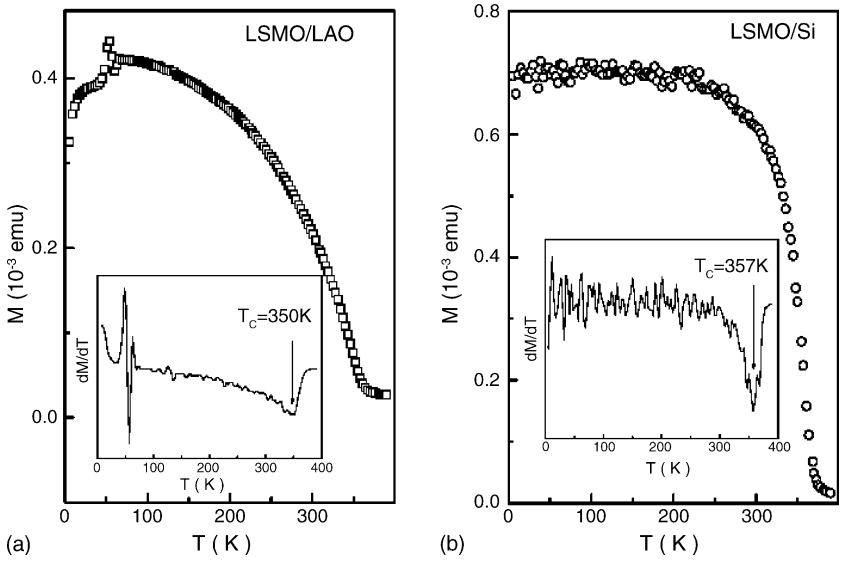

Fig. 6. The temperature dependence of magnetization $M(T)$ for LSMO/LAO film (a) and the LSMO/Si film (b) at $H = 0.1$ T. The inset is the corresponding plot of dM/dT vs. temperature.

thought to be strong link. In contrast, the LSMO film on the Si substrates [Fig. 5(b)] has porous GBs that are thought as weak link by Wang et al. [12,18].

The temperature dependence of magnetization $M(T)$ of LSMO/LAO and LSMO/Si films under an applied field of 0.1 T perpendicular to the film surface under zero-field-cooling (ZFC) mode is shown in Fig. 6(a) and (b), respectively. The LSMO/LAO film shows a paramagnetic (PM) to ferromagnetic (FM) transition at the Curie temperature T_C of 350 K (defined as the temperature where dM/dT is minimum as shown in the inset of Fig. 6(a)). A little anomaly of magnetic moment at about 50 K is suggested to be ascribed to the appearance of a small amount of the Mn_3O_4 impurity phase [19,20]. For the LSMO/Si film, T_C is 357 K as shown in inset of Fig. 6(b), which is slightly higher than that of the LSMO/LAO film.

The magnetic field dependence of MR for LSMO/LAO and LSMO/Si films at different temperatures is shown in Fig. 7(a) and (b), respectively. For the LSMO/LAO film, Fig. 7(a) shows that there exists a remarkable decrease of resistance with increasing applied fields only in the vicinity of T_C (~350 K). At low temperatures far from T_C, such as 200 and 5 K, the resistance shows a very slow drop with the increase of applied fields. The MR behavior is of the typical characteristic of epitaxial CMR films, which indicates that the LSMO/LAO film is epitaxial without weak link GBs. By

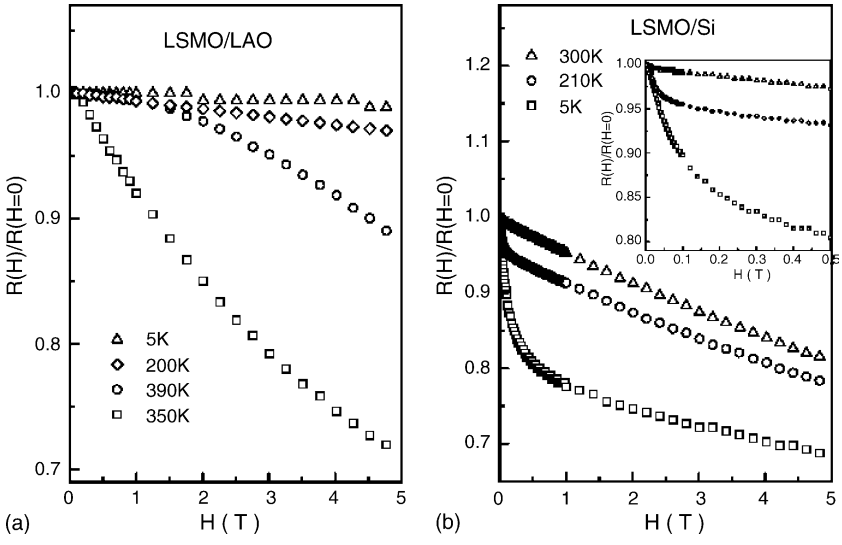

Fig. 7. The magnetic field dependence of the normalized resistance at various temperatures for LSMO/LAO film (a) and the LSMO/Si film (b). The inset of (b) is the amplified plot at the low field below 0.05 T.

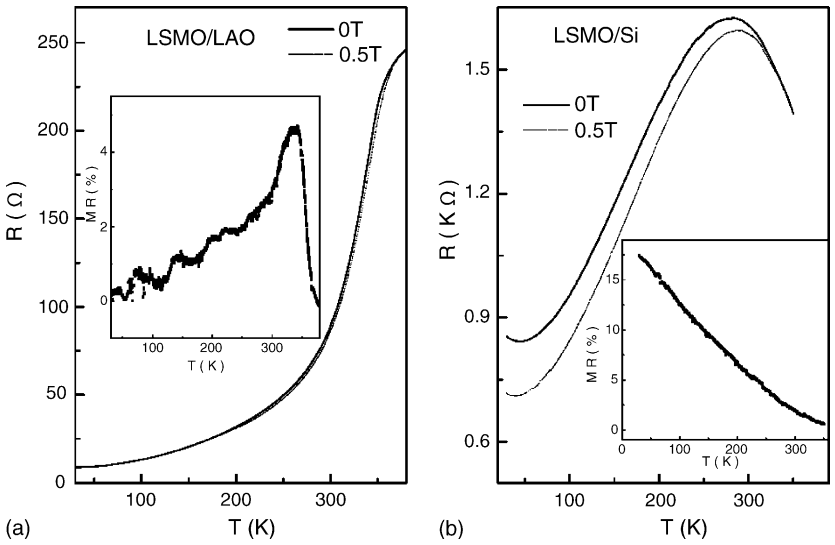

Fig. 8. The temperature dependence of resistance for LSMO/LAO film (a) and the LSMO/Si film (b). The inset is the corresponding plot of MR vs. temperature.

contrast, the LSMO/Si exhibits an obvious MR effect in the whole measured temperature range as shown in main panel of Fig. 7(b). Especially, its LFMR is remarkably enhanced at low temperatures as shown in inset of Fig. 7(b).

The temperature dependence of the resistance at $H = 0$ and 0.5 T for LSMO/LAO and LSMO/Si films is shown in Fig. 8(a) and (b), respectively. It shows that the temperature at the maximum resistance, T_P, of the LSMO/LAO film is higher than that of the LSMO/Si film. The temperature dependence of MR of LSMO/LAO and LSMO/Si films are shown in the inset of Fig. 8(a) and (b), respectively. For the LSMO/LAO film, it exhibits that there exists an obvious peak only near T_C and the MR decreases continuously with decreasing temperatures. The results suggest that the MR of the LSMO/LAO film mainly originates from the suppression of spin fluctuation within grains and the GBs do not contribute to MR [21]. In contrast, for the LSMO/Si film, the MR increases with decreasing temperature, which is suggested to stem from spin-dependent scattering of polarized electrons at the GBs [9].

4. Conclusion

In summary, LSMO films were successfully fabricated on Si (1 0 0) and $LaAlO_3$ (1 0 0) single crystal substrates by CSD method. It was found that the substrates played an important role on the structural, magnetic and transport properties of the LSMO films. The LSMO/Si film behaved as the characteristic of the polycrystalline film, whereas the LSMO/LAO film exhibited the properties similar to those of the single crystalline and the epitaxial film. The MR of the LSMO/Si film was largely enhanced at low temperatures compared with that of the LSMO/LAO film. The difference of MR properties was ascribed to the grain boundary effects.

Acknowledgments

This work was supported by the National Superconductivity 863 project under No. 2002AA306211, No. 2002AA306281, the National Nature Science Foundation of China under contract No. 10174085, No. 2004AA306130 and No. 10374033, Anhui Province NSF Grant No. 03046201 and the Fundamental Bureau Chinese Academy of Sciences.

References

[1] Z. Trajanovic, C. Kwon, M.C. Robson, K.C. Kim, M. Rajeswari, R. Ramesh, T. Venkatesan, Appl. Phys. Lett. 69 (1996) 1005–1007.
[2] K. Chahara, T. Ohno, M. Kasai, Y. Kozono, Appl. Phys. Lett. 63 (1993) 1990–1992.
[3] J. Inoue, S. Maekawa, Phys. Rev. Lett. 74 (1995) 3407–3410.
[4] S. Jin, T.H. Tiefel, M. McCormack, R.A. Fastnacht, R. Ramesh, L.H. Chen, Science 264 (1994) 413–415.
[5] R. Shreekala, M. Rajeswari, K. Ghosh, A. Goyal, J.Y. Gu, C. Kwon, Z. Trajanovic, T. Boettcher, R.L. Greene, R. Ramesh, T. Venkatesan, Appl. Phys. Lett. 71 (1997) 282–284.
[6] J. Gao, S.Q. Shen, T.K. Li, J.R. Sun, Appl. Phys. Lett. 82 (2003) 4732–4734.
[7] R. Desfeux, S. Bailleul, A. Da Costa, W. Prellier, A.M. Haghiri-Gosnet, Appl. Phys. Lett. 78 (2001) 3681–3683.
[8] I.B. Shim, H.M. Lee, K.T. Park, B.W. Lee, C.S. Kim, J. Magn. Magn. Mater. 242–245 (2002) 1169–1171.
[9] X.W. Li, A. Gupta, G. Xiao, G.Q. Gong, Appl. Phys. Lett. 71 (1997) 1124–1126.
[10] S.Y. Bae, S.X. Wang, J. Mater. Res. 13 (1998) 3234–3240.
[11] A.M. Haghiri-Gosnet, J. Wolfman, B. Mercey, Ch. Simon, P. Lecoeur, M. Korzenski, M. Hervieu, R. Desfeux, G. Baldinozzi, J. Appl. Phys. 88 (2000) 4257–4264.
[12] X.L. Wang, S.X. Dou, H.K. Liu, M. Ionescu, B. Zeimetz, Appl. Phys. Lett. 73 (1998) 396–398.
[13] N.D. Mathur, G. Burnell, S.P. Isaac, T.J. Jackson, B.S. Teo, J.L. MacManus-Driscoll, L.F. Cohen, J.E. Evetts, M.G. Blamire, Nature (London) 387 (1997) 266–268.

[14] A. Gupta, G.Q. Gong, G. Xiao, P.R. Duncombe, P. Lecoeur, P. Trouilloud, Y.Y. Wang, V.P. Dravid, Phys. Rev. B 54 (1996) R15629–R15632.
[15] F.X. Cheng, Z.Y. Peng, Z.G. Xu, C.S. Liao, C.H. Yan, Thin Solid Film 339 (1999) 109–113.
[16] Z.L. Zhang, Z.M. Wang, Y.H. Huang, F.X. Cheng, C.S. Liao, S. Gao, C.H. Yan, Chem. J. Univ. 20 (1999) 665–669 (in Chinese).
[17] Y.P. Lee, S.Y. Park, V.G. Prokhorov, V.A. Komashko, V.L. Svetchnikov, Appl. Phys. Lett. 84 (2004) 777–779.
[18] H.K. Singh, N. Khare, P.K. Sinach, O.N. Strivastava, J. Phys. D: Appl. Phys. 33 (2000) 921–925.
[19] G. Dezanneau, A. Sin, H. Roussel, H. Vincent, M. Audier, Solid State Commun. 121 (2002) 133–137.
[20] J.W. Cai, C. Wang, B.G. Shen, J.G. Zhao, W.S. Zhan, Appl. Phys. Lett. 71 (1997) 1727–1729.
[21] H.Y. Hwang, S.W. Cheong, N.P. Ong, B. Batlogg, Phys. Rev. Lett. 77 (1996) 2041–2044.